JOURNAL OF PROPULSION AND POWER
Vol. 24, No. 3, May–June 2008

Laboratory Scale Survey of Pentad Injector Stability Characteristics

Ryan C. Cavitt* and Robert A. Frederick Jr.†
University of Alabama in Huntsville, Huntsville, Alabama 35801
and
Vladimir G. Bazarov‡
Moscow Aviation Institute, 125993, Moscow, Russia

DOI: 10.2514/1.32618

This work provides an assessment of an experimental method for characterizing combustion stability of liquid rocket injectors. The research has shown that the single-element laboratory scale methodology is capable of creating high-frequency combustion instability with gaseous methane and oxygen. Modified pentad impinging jet injectors were selected for the stability survey. The maximum peak-to-peak dynamic pressure recorded in the chamber was 27% of the mean chamber pressure. Other factors indicating instability include injector manifold pressure pulsations as well as twofold chamber temperature increases from steady operation. The testing evidenced that the flame structure varies with the onset of unstable combustion as well as mode transition. Moreover, a bifurcation process was seen as the dominant frequency shifted. The results also showed that there were significant differences in stability characteristics which were a function of fuel impingement angle. Correlation with chamber natural frequency predictions suggest that the injectors excited the first radial mode and the first radial, second tangential combined mode.

I. Introduction

HIGH-FREQUENCY combustion instability, or acoustic instability, is a coupling of the combustion process and the system fluid dynamics [1,2]. In attempts to eliminate high-frequency combustion instability, engine component modifications or additions can be used, for both passive and active control. To increase engine stability, the injector characteristics are often altered. The injector plays a key role because it is the connection between the feed system and combustion chamber. The injector's importance is evident from years of research and the prime example of the F-1 engine development [3]. Computational techniques for predicting instability are becoming more proficient, but still rely heavily on experimental results. An experimental laboratory scale technique that is capable of predicting qualitative and quantitative injector stability characteristics would greatly improve the confidence of stability in an initial full-scale engine test program.

Recent publications describe a laboratory scale test methodology that may quickly provide a means to produce crucial experimental data developers have been searching for [4–6]. The methodology employs an injector screening apparatus which determines the injector stability characteristics. The test methodology is attractive from the engine development standpoint by saving both valuable time and resources. With the proper injector manifold design, many injector designs can be tested in rapid succession, saving critical development time. To reduce resources, the scaling approach allows the test facility to be run with gaseous propellants at modest flow rates.

Throughout the history of high-frequency combustion instability research, many theories have been developed [7,8]. Most theories identify the time delay between injection and combustion to be the dominant factor controlling combustion stability. Three major mechanisms have been repeatedly identified to control this delay: atomization, vaporization, and propellant mixing. The underlying assumption of this methodology is that mixing is the dominant process leading to high-frequency combustion instability. This assumption is accurate for engines with high chamber pressure and staged combustion cycles. With sufficiently high pressure and temperature of the propellants entering the injector, supercritical propellant conditions are approached or achieved. Therefore, surface tension is absent, which negates consideration of atomization and vaporization.

The absence of surface tension significantly simplifies the requirements for laboratory scale testing, but the process of scaling the operating conditions of a full-scale engine operating near or above supercritical conditions is still not a simple task. In fact, for most cases, it is impossible to match all appropriate criteria. Therefore, this methodology applies approximate scaling to the engine. It is critical to identify the correct scaling condition for the injector under investigation. Possible parameters which may control the mixing process include Reynolds number, Euler number, momentum ratio, and propellant kinetic head. Additional basic scaling criteria must be set equal between the full-scale engine and model. These criteria include injector physical dimensions, volumetric flow rate, chamber natural frequency, and wavelength of the injector channels. The final consideration is combustion chemistry. It is assumed that the equivalence ratio must also be similar from subscale to full-scale conditions. The test apparatus calls for gaseous propellants, which most closely represent supercritical fluids, and the combustion chamber pressure is kept nearly atmospheric. This allows long duration firings under low absolute oscillation amplitudes to minimize hardware damage. The amplitudes are insignificant with respect to absolute magnitude, but can be significant in relation to the atmospheric chamber pressure.

In the past decade, this methodology has been described in the open literature by Russian and Korean researchers [4,5]. A definitive description of the methodology has been produced by the Russian

Presented as Paper 5587 at the 43rd AIAA/ASME/SAE/ASEE Joint Propulsion Conference & Exhibit, Cincinnati Duke Energy Convention Center, Cincinnati, OH ; received 4 June 2007; revision received 8 January 2008; accepted for publication 11 January 2008.

*Propulsion Engineer, Orbital Technologies Corporation, 1212 Fourier Drive, Madison, Wisconsin 53717. AIAA Member.

†Assistant Director, University of Alabama in Huntsville Propulsion Research Center, 5000 Technology Drive. AIAA Associate Fellow.

‡Visiting Eminent Scholar of Propulsion, University of Alabama in Huntsville Propulsion Research Center, 5000 Technology Drive. AIAA Member.

test facility where the testing procedure originated [6]. The author indicates that model firings have been successful in increasing the stability of the 4D75 and 15D79 engines [6]. Furthermore, the methodology has been validated at the facility by correlating full-scale and laboratory scale data. External to the originating facility, the methodology has been applied to multiple injector types at Korea Aerospace Research Institute. Testing with coaxial swirl injectors was shown to have increased stability with decreased recess ratio, which is a similar stability trend obtained by other test methods [9]. The scaling technique was also applied to a split triplet impinging jet injector which showed significant differences in stability with respect to geometric injector characteristics [10].

The experimental survey presented is an application of this scaling methodology. A single-element test facility has been assembled and assessed with several pentad injectors. The initial test program was successful at creating high-frequency combustion instability with the relatively simple test apparatus. The results are a map which shows the magnitude of pressure oscillations as a function of injector operating conditions for three injector configurations. The survey described is not an application of the scaling procedure to any specific engine. The selected injector was selected due to the likeliness of experiencing instability. There are currently no full-scale data to compare the laboratory scale results against. Correlation of measured and predicted frequencies indicate that the test program was capable of exciting transverse modes of instability rarely found in the research field at the laboratory scale.

II. Experiment Description

A. Experimental Approach

The primary objective of the testing was to produce spontaneous high-frequency combustion instability. Therefore, a unique type of pentad injector was selected for the study based on the probability of experiencing acoustic instability. The injector is typical of Russian military engines using hypergolic propellants. One of the injectors tested can be seen in Fig. 1. The secondary objective of the survey was to study one injector variable, namely, the angle at which the fuel is injected into the oxygen flow. Therefore, two other impingement angles were tested: 30 deg (fuel spray impingement farthest from the injection site) and 60 deg (fuel spray impingement closest to the injection site). All linear and diametral dimensions shown in Fig. 1 were consistent for all injectors.

This injector is unconventional in the location at which the propellants intersect. The fuel (methane) is impinging the central oxidizer (oxygen) inside of the oxidizer post itself. Typical impinging jet injectors intersect downstream of the fire face in the chamber, not within the injector tip. This aspect of the injector makes determination of the fuel pressure drop a function of multiple operating parameters, namely, the mass flow rates of both the fuel and oxygen. As the propellants were throttled significantly, the associated pressure drops ranged between 5 and 35% of the chamber pressure.

The test matrix used for the survey is shown in Fig. 2. The propellants are pure gaseous methane and pure gaseous oxygen. There was no inert dilution or heating of the propellants. A single test consisted of a constant methane mass flow rate. The oxygen mass flow rate was increased from rich to lean combustion chemistry. For each test there were 13 set points: 6 rich, 6 lean, and 1 stoichiometric. To achieve all 13 set points, the firing duration for a single test was approximately 2 min. This process was repeated for nine methane mass flow rates. The equivalence ratio range from test to test was consistent at 2–0.5. This is the reason for the odd triangular shape of the test matrix. To aid in ascertaining the repeatability of the experiment, the test matrix was run on each injector on four separate occasions.

B. Test Facility

A piping and instrumentation diagram of the experiment can be seen in Fig. 3. All of the instrumentation and hardware is mounted to a cart which is supplied with propellants via a preexisting rocket test

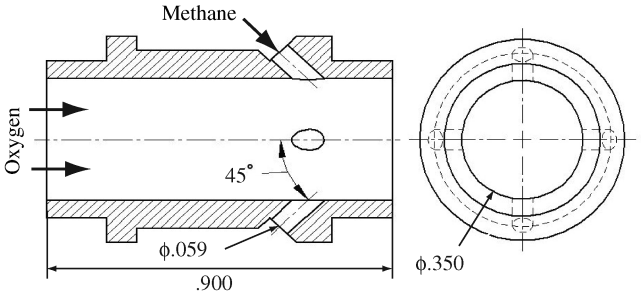

Fig. 1 Forty-five degree impinging jet injector (dimensions in inches).

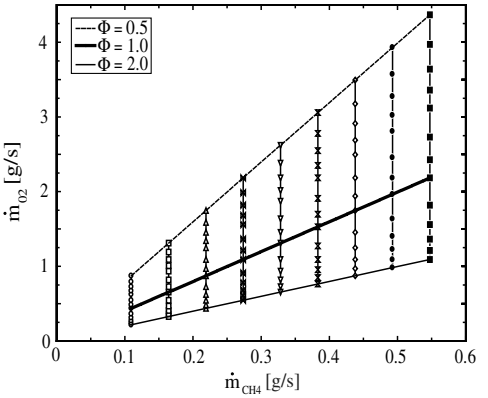

Fig. 2 Stability mapping test matrix.

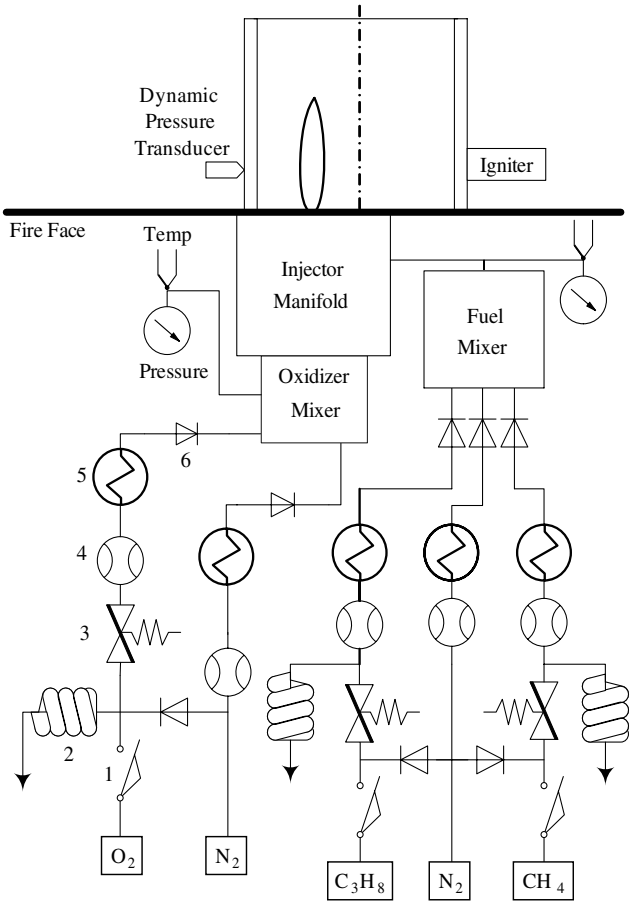

Fig. 3 Test facility piping and instrumentation schematic: 1) fire valve, 2) relief valve, 3) pressure regulator, 4) mass flow controller, 5) heating element, 6) check valve.

stand feed system. The experiment is controlled remotely from the facility control room. The atmospheric pressure chamber is an 8 in. cylinder without a converging section. The chamber is sealed to a fire face to prevent mean flow into the chamber from the atmosphere. For the results presented here, the single injector is placed 2.5 in. from the chamber wall. This location was selected due to the restrictions of the uncooled chamber. Assuming that the injector responds more strongly to pressure pulsations than velocity pulsations, it would be ideal to place the injector at the wall to investigate the tangential mode, and at the center of the chamber to excite the radial mode. The injector cover is installed flush to the fire face. The modular injector manifold allows many types of injectors to be tested besides those described here, including coaxial swirl and shear coaxial injectors.

The feed system has enhanced flow capabilities beyond that of a typical test stand. The oxidizer is gaseous oxygen which can be diluted with nitrogen to vary volumetric flow rate without changing combustion chemistry. The fuel side has capabilities for two simultaneous fuels, methane and propane, with a similar diluent capacity. Each of the feed lines has common equipment. The mass flow controller allows throttling of any gas flow during testing. There is also a heating element in each feed line which further expands volumetric flow rate capability as well as variation of propellant speed of sound. Typical static pressure and temperature measurements were taken in the feed system, including manifold pressure and temperature.

The nature of the experiment calls for many measurements of the chamber conditions. By placing the injector asymmetrically in the chamber, a complex thermal and therefore acoustic field is present. Determining the thermal environment is a crucial step to correlate the experimental frequencies to the natural frequency for the chamber without the aid of multiple high-frequency pressure transducers. Therefore, the chamber was instrumented with an array of five thermocouples to quantify the temperature gradient. The array was equally spaced around half of the chamber circumference, and axially 2 in. from the fire face. No static pressure measurements were taken and dynamic pressure readings were taken with a single water-cooled dynamic pressure transducer. This transducer was also placed 2 in. from the fire face. Optical data were taken with a standard video camera. Continuous monitoring of the flame was recorded for each test because there was no nozzle restricting view. This feature is convenient in monitoring the structure of the flame from stable to unstable operation as well as transitions in modes. The injector was ignited with a hydrogen/oxygen spark augmented igniter. A frame extracted from the test footage can be seen in Fig. 4. The chamber dynamic, water-cooled pressure transducer, igniter, and thermocouple array can be seen in the photograph. Details of the test facility and experimental test matrix can be found in [11].

The test matrix called for 13 oxygen mass flow rate set points per test. At each set point, the dynamic pressure transducer measurement was recorded. This signal was sampled at 150 kHz and channeled through a Butterworth antialiasing filter. The time domain signal was then transferred to the frequency domain by fast Fourier transform (FFT).

Figure 5 illustrates how the FFT data were analyzed for stability mapping. The most important analysis factors for the subsequent results are the maximum amplitude and corresponding peak frequency at each set point. Algorithms were created to search for the maximum amplitude and frequency within a defined frequency bandwidth for each set point. However, the power density must also be considered. Peaks can differ in width from mode to mode. By integrating across the frequency domain, the total power density was also determined. The algorithm also searched for peaks above a defined pressure threshold as well as the power density within the peaks. The development of the algorithm was necessary for subsequent stability mapping.

III. Results and Discussion

A. High-Frequency Combustion Instability

The fundamental goal of the test program was to demonstrate conditions where high-frequency combustion instability occur.

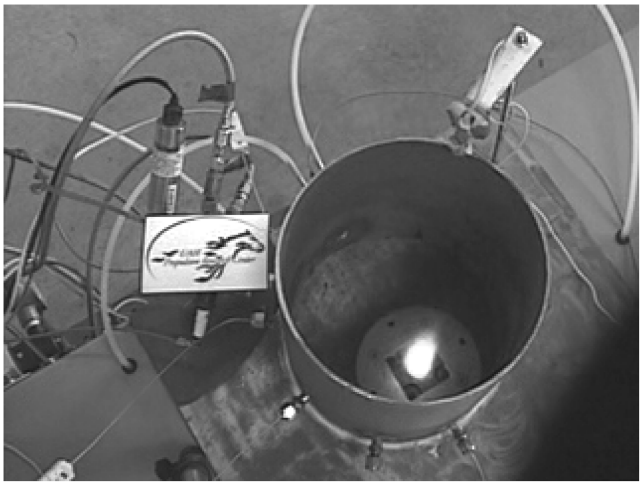

Fig. 4 Example of apparatus during experimentation.

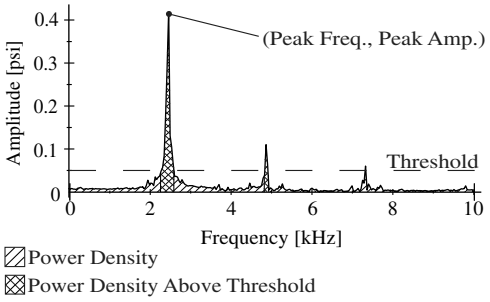

Fig. 5 Fourier transform analysis.

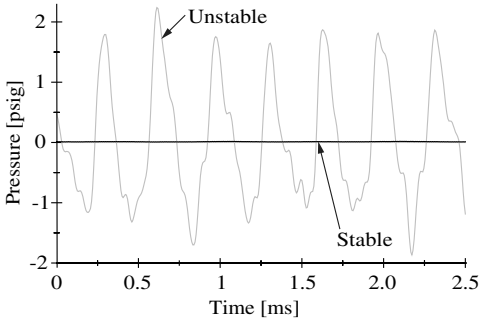

Fig. 6 Sample dynamic pressure signals.

There were multiple experimental indications of high-frequency combustion instability. These included periodic high-amplitude dynamic chamber pressure, increased heat release in the chamber, as well as pressure oscillations in the injector manifold. All of these phenomena were present in the injector survey experimentation [11].

A sample of the dynamic pressure signals recorded can be seen in Fig. 6. The flat, stable signal was typical for steady operating conditions during experimentation at the most fuel-rich set point. Although low-amplitude oscillations may be present in high-pressure chambers at natural frequencies, similar pulsations were not detectable in the atmospheric burner. The unstable signal shows fairly smooth oscillation, which indicates sufficient sampling rate, typical of lean conditions at 0.328 g/s of methane. There is an obvious fundamental mode with harmonics. The pressure oscillations were expected to be nearly sinusoidal with the atmospheric pressure chamber. High-pressure chambers typically experience sawtooth-shaped waves, and the experimental results are more closely approximated by linear acoustics, which leads to a smoother signal. Ignoring the harmonics, the peak-to-peak pressure

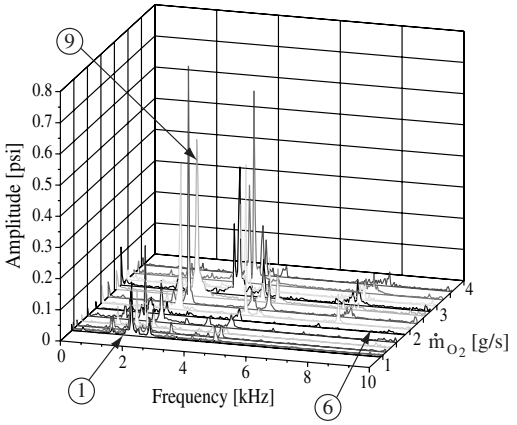

Fig. 7 Sample waterfall plot.

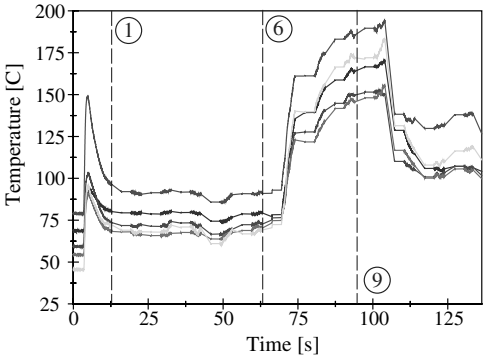

Fig. 8 Sample chamber temperature plot.

is approximately 3.5 psi, which is 24% of the mean chamber pressure. This magnitude is far beyond common unstable thresholds.

As an example of the results for a single test, a waterfall plot can be seen in Fig. 7. The waterfall plot is for a constant fuel mass flow rate of 0.438 g/s and 13 oxygen mass flow rates as described in Sec. II.A. As the oxygen mass flow increases, the dominant frequency distinctly transitions twice. The initial frequency is low amplitude in the 2000 Hz range. The first shift is to 2500 Hz and, finally, near 3800 Hz. The final two zones have significantly larger amplitudes than the first region. It should also be noted that the peaks in the lean region have wider bandwidths than the previous two zones.

The experimentation also showed significant chamber temperature increases at the onset of high-amplitude pulsations. A plot of the five chamber temperatures can be seen in Fig. 8. These data were taken from the same test as Fig. 7. Unfortunately, there are gaps in the data, represented as straight lines due to the data acquisition system switch required for high-frequency pressure acquisition. The temporal data can be correlated to Fig. 7 by the set points. The vertical dashed lines identify the time that the high-frequency measurement was sampled, with the corresponding set point number. The temperature plot also shows three distinct regions. The chamber temperatures nearly double between the sixth and seventh set points which directly corresponds the waterfall frequency shift. A significant decrease in temperature between the 10th and 11th set points is also present.

The manifold pressures from this test can be seen in Fig. 9. The vertical, dashed lines again correlate to the high-frequency pressure sampling time for the set point. The pressures represented here were taken with static pressure transducers. The graph depicts the injector's pressure drop characteristics. The fuel manifold pressure must increase to maintain a constant mass flow rate as the oxygen mass flow rate increases. Although quantitative dynamic information cannot be taken from the data, qualitative trends can be seen. Under stable conditions, the injector pressure has negligible variation, typical of any turbulent process. Again, between the sixth and

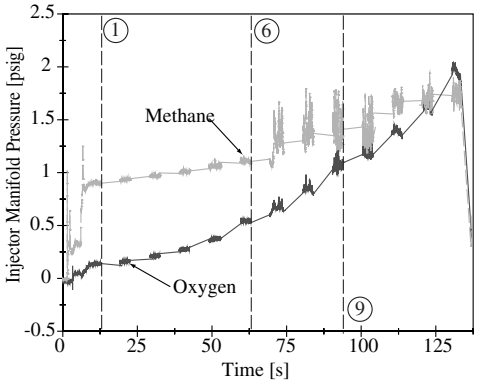

Fig. 9 Sample injector manifold pressure plot.

seventh set point, manifold pressure unsteadiness can be seen, especially in the fuel manifold. The second shift is present between the 10th and 11th set point in the fuel manifold as the unsteady amplitude decreases. The second frequency shift shown between the ninth and 10th set points in the waterfall plot is present in the chamber temperature and manifold pressure, but between the 10th and 11th set points. This disparity is potentially due to the high-frequency sampling timing and duration as well as the violent flame behavior during the frequency shift.

The video footage of the this sequence revealed interesting flame structure transitions. As anticipated, the flame was vertical for steady operation. When the system was unstable at 2500 Hz, the flame bent toward the center of the chamber. This frequency was the most prevalent as well as the highest in amplitude found throughout the test program. The other high-amplitude frequency was 3800 Hz. The flame structure of this mode was much different. First, because the frequency appeared at lean conditions, the flame was much shorter. Second, the flame bent 90 deg in the fire face plane from the 2500 Hz mode. As shown in the sample plots, a single test was capable of exciting both modes at different oxygen mass flow rates. The transition between modes was not smooth. A bifurcation region was present where the flame randomly switched between the two modes without changes in the nominal propellant flow rates. This result shows that there is significant flame reaction to the mode of instability as well as a chaotic and violent transition between modes.

B. Instability Mode Determination

Because there was only one pressure transducer, some approximations were used to estimate the mode of instability observed. Natural frequency calculations based on the recorded chamber temperatures were necessary to identify the excited mode of instability. The uncertainty related to the correlation could be eliminated through expanding the instrumentation to multiple transducers.

A graph of the experimental peak frequencies from a single test and the predicted chamber natural frequencies can be seen in Fig. 10. The results shown here are not from the same test as the sample plots in Sec. III.A.

The first and second set point closely correlate to the second tangential mode. The third set point transitions to the first radial mode and back for the fourth. The rest of the set points closely correlate to the first radial mode. In general, there is excellent agreement between the predicted and experimental modes. The test shown in Fig. 10 exhibits high-amplitude pulsations between the 7th and 13th set point. The predicted modes shift up with the increase in temperature, which is consistent with the shift in the experimental data. It must also be noted that the prediction is low in the high-amplitude region due to the location of the thermocouples in the chamber. The probes protrude through the wall 0.1 in., and so the reported temperatures are assumed to be low. This underestimation was not compensated for because assumptions on the gas composition were already implemented to complete the calculation. In general, based on the calculated natural frequencies, the first radial mode was near

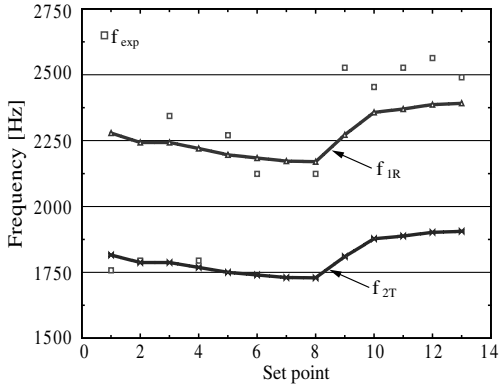

Fig. 10 Correlation of measured peak frequency and predicted chamber natural frequency.

2500 Hz, whereas the first radial, second tangential combined mode was near 3800 Hz. The location of the injector gives further credibility to the correlated frequencies. The injector was placed 2.5 in. from the chamber wall, and therefore 2.5 in. from the tangential pressure antinode. With an 8-in.-diam resonator, the injector is located 1.5 in. from the chamber centerline. The chamber centerline is where the radial mode antinode resides. Therefore, the injector was placed closer to the first radial pressure antinode than the first tangential pressure antinode. This observation lends further probability to the identification of the first radial mode of instability at 2500 Hz.

C. Stability Mapping

By applying stability mapping, the most troublesome areas of high amplitude instability can be defined. The goal of such data representation is to quantify how far a possible nominal full-scale operating condition is from unstable combustion. Because this work was not completed under a developmental project, a survey of the stability is presented.

The algorithm previously described was capable of finding the maximum FFT amplitude at each test matrix set point. The stability map amplitudes presented are from the maximums of the FFTs, not the time domain signals. The amplitudes describe the peak pressure of the fundamental mode alone. This pulsation strength representation is conservative because the maps are created from the peak pressure of the fundamental mode without the harmonics. The peak-to-peak time domain signal is significantly higher than the fundamental mode amplitude in most cases. To create the two-dimensional maps, interpolation was required to make a coherent contour. Embedded MATLAB functions were used to allow proper data representation. Grid generation studies were also employed to ensure proper interpolation of the amplitude data. The traditional stability map has a defined amplitude threshold which is considered unstable. The mapping technique applied here has no threshold; each test matrix set point has an associated amplitude. The amplitudes presented in this section are the maximums from four separate test sessions. The axes for the plots are the volumetric flow rate of the propellants, oxygen and methane. The plots are similar to Fig. 2, differing only by the manifold gas density, which was nearly constant even up to the higher flow rates.

Figure 11 is the stability map for the 30 deg impinging jet injector. The high amplitude instability area is in the central, lean region. This is the zone where the radial mode was prevalent. The combined mode region is in the upper right-hand corner of the graph at lean, high volumetric flow rates. One interesting aspect of the graph is the near absence of instability in the rich region. Also, the onset of instability to the central region is fairly steep when approaching from the rich zone.

The 45 deg stability map in Fig. 12 shows similar results. The modes excited are in similar regions. The major difference is in the significant growth of the central region. There is also a high-amplitude region centered at 350 cm^3/s of methane and 600 cm^3/s of oxygen.

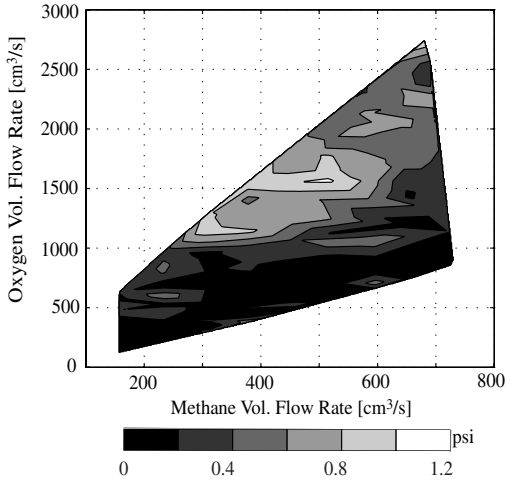

Fig. 11 Thirty degree impinging jet maximum amplitude stability map.

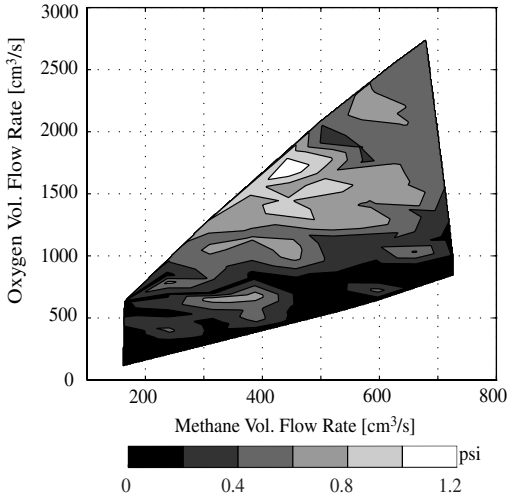

Fig. 12 Forty-five degree impinging jet maximum amplitude stability map.

The 60 deg impinging injector shows a much different picture, as shown in Fig. 13. The central region is shifted up and to the right. Actually, the radial mode region only exists as the peak at 450 cm^3/s of methane and 1750 cm^3/s of oxygen. The combined mode region in the upper right-hand corner is of stronger amplitude than the other injectors.

D. Mode Mapping

The application of stability mode mapping has multiple advantages. The first advantage is if the nominal operating conditions are near a region of instability, the mode can be identified. The second is if there are multiple modes present, the transition regions can be identified. This is important if the nominal flight operation is near an area of transition. If the injector design is already finalized, acoustic absorption devices may be required. This technique will show if the devices need to be tuned to a single frequency or multiple.

By searching the FFTs at smaller bandwidths for maximum amplitudes, it is possible to determine which modes are excited at each experimental set point. The frequencies mentioned previously are the frequencies that were searched for in the mode mapping. The average radial mode frequency was at 2500 Hz, and so the radial mode was searched for between 2000 and 3000 Hz. The average first radial mode, second tangential combined mode was at 3800 Hz, and so the amplitudes were searched between 3300 and 4300 Hz. The

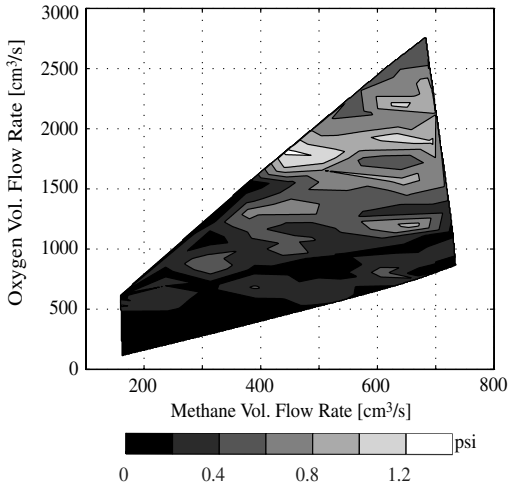

Fig. 13 Sixty degree impinging jet maximum amplitude stability map.

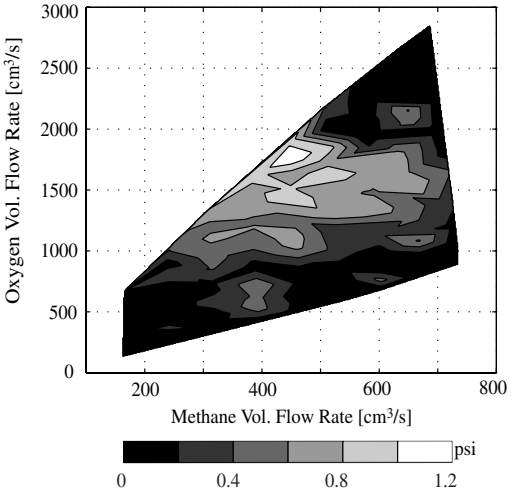

Fig. 14 Forty-five degree impinging jet: first radial mode.

amplitudes reported are from the maximum of all four test sessions. Only the results from the 45 deg impinging jet injector are presented. The mode separation characteristics are similar for the other injectors investigated.

Figures 14 and 15 depict the regions affected by different modes of instability. The first radial mode is certainly the most active in the lean, moderate methane flow region. This mode of instability was not anticipated with the experimental planning. From the previously described injector placement with respect to the chamber acoustic field, it is possible to justify the mode of excitation as the radial mode. With the velocity perturbation 90 deg out of phase with the pressure, it is shown that the injector stability is excited by pressure pulsation rather than velocity pulsation.

Figure 15 is the maximum amplitude for the first radial, second tangential combined mode. In the bandwidth searched, there is no amplitude in excess of 0.2 psi below 1500 cm^3/s of oxygen. This shows that the combined mode is truly only present in the lean, high-energy release region.

By comparing the two graphs, it is possible to see the overlapping region centralized at 1750 cm^3/s of oxygen. This is the region in which the bifurcation transition is present. This process is rather violent and is difficult to make a clear distinction within reasonable experimental uncertainty which mode is present because, for a single set of nominal operating conditions, multiple modes exist.

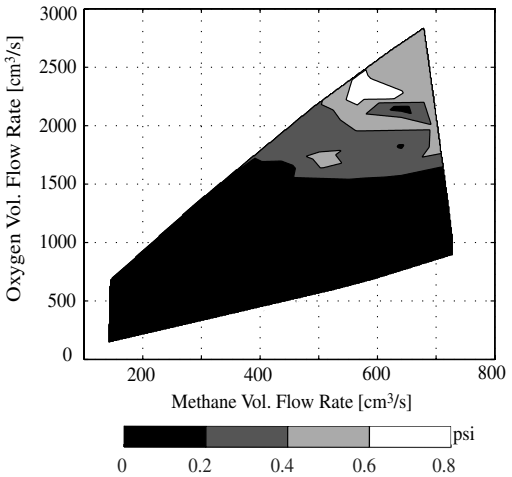

Fig. 15 Forty-five degree impinging jet: combined first radial, second tangential mode.

E. Repeatability and Variability

To describe the process variability and repeatability, the average amplitude of each set point was taken for four test sessions. Figure 16 is the stability map for the 45 deg injector plotted with the average amplitudes.

The comparison of the average map and Fig. 12 illustrates the experimental repeatability. The first difference to note is the change in contour amplitudes. The average contour maximum at 0.8 psi must be increased by 150% to match 1.2 psi in the maximum amplitude map. This shows that from test session to test session there was a deviation in the strength of the pulsations present. Another feature to note is the overall shape of high-amplitude regions. By averaging the amplitudes and producing similar high-amplitude shapes, it is confirmed that the spontaneous instabilities were excited in nearly the same region on different test periods. The final point to note on variability is the region in which the injector transitions from the first radial to the first radial, second tangential combined mode. This region is difficult to map and is confirmed by comparison of the maps from each separate test session. The source of the differentiation between nominally identical tests was not identified.

By looking at the injectors at a set equivalence ratio, it is possible to highlight the differences in stability for the three injectors. Figure 17 shows the results for all three injectors at a set equivalence ratio of 0.58 and varying total mass flow rate. This equivalence ratio was selected because lean conditions were found to be unstable.

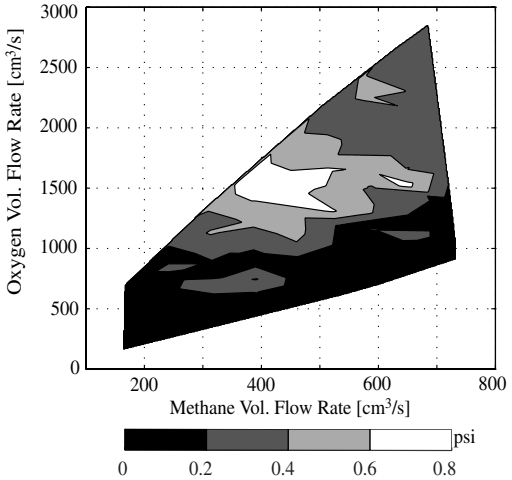

Fig. 16 Forty-five degree impinging jet average amplitude.

The 30 deg injector rises and falls as the total mass flow rate is increased. This is a result of the high-amplitude radial instability in the central region of the stability maps. The 45 deg injector shows a very similar trend to the 30 deg injector. The main difference is the tapering of amplitude above 3.25 g/s. The amplitude level is a result

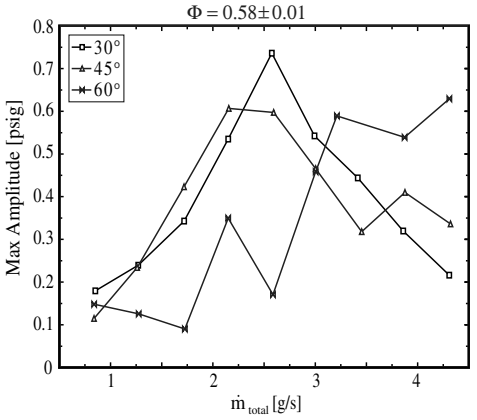

Fig. 17 FFT maximum amplitude comparison $\Phi = 0.58$.

of the excitation of the combined first radial, second tangential mode. The 60 deg injector, again, has a much different trend. The amplitude rises with increased mass flow rate and levels out above 3 g/s. This is due to the tendency of this injector to become unstable at the combined mode rather than the pure radial mode.

The energy density results supported the conclusions from the FFT pressure amplitude plots. Mapping of the energy density showed that the combined mode holds significant energy due to the width of the peaks. To further support the results, the energy did not simply scale up with the fuel mass flow rate. If the energy was simply due to the increase in available energy from the increased fuel flow rate, the energy would consistently increase to the highest fuel flow rate. The energy increases in similar locations to the peak pressure amplitude, with the exception that the combined mode has a nearly equivalent energy amplitude. The transition region is level with the radial and combined mode peaks.

Without the application of analytical or numerical techniques to support the work, it is impossible to strictly determine the mechanism for the onset of instability in the experiment. The presence of the instability is thought to be in part from the vigorous mixing that is inherent to the fuel injection technique. From examination of the flame at various equivalence ratios, it is apparent that the flame was not detached from the injector tip. This indicates that the propellants were sufficiently mixed to combust immediately in the chamber or in the injector tip itself. The mechanisms most likely to induce instability are represented as a delay between injection and combustion, in this case, the mixing time. This fact makes sense when evaluating the typical use of the injector, hypergolic propellant that does not mix as easily as the gaseous methane and oxygen. The mixing delay is accompanied by the injector coupling as an unstable reinforcement mechanism. The connection between the chamber and the feed system is illustrated by the manifold pulsations. Without proper instrumentation, the phase, amplitude, and frequency of the pulsations could not be determined to elucidate the connection. The relatively low-pressure drops indicate that the feed system was not properly isolated from the chamber at all conditions.

IV. Conclusions

A subscale test facility has been designed and fabricated to employ a scaling technique which allows the liquid rocket engine designer to determine injector stability characteristics early in the design phase of a development program. A survey of high-frequency combustion instability injector characteristics has been completed with the test bed. For this study, a modified pentad configuration was employed. Multiple fuel impingement angles were tested to identify differences in stability as a function of impingement angle. The gaseous methane and gaseous oxygen mass flow rate were varied to create a coherent representation of the injector stability over a wide range of operating conditions.

The experimentation has shown that application of the scaling methodology is capable of creating high-frequency combustion instability. Typical results include injector manifold pressure pulsations, increased chamber heat release, and smooth chamber pressure pulsations. By employing an open chamber, observing flame structure under all test conditions was possible. The onset of the first radial mode was evident by a bending of the flame. Transition regions were present at certain operating conditions. These regions have a bifurcation between the first radial and the combined first radial, second tangential modes, which were evident by violent flame flipping accompanied with the change in audible frequency. It has also been shown that the fuel impingement angle of the fuel has a significant effect on the injector stability characteristics.

References

[1] Coultas, T. A., "Combustion Instability," *Liquid Propellant Rocket Combustion Instability*, edited by D. T. Harrje, and F. H. Reardon, NASA, SP-194, 1972, pp. 14–29.

[2] Yang, V., and Anderson, W. E. (eds.), *Liquid Rocket Engine Combustion Instability*, Progress in Astronautics and Aeronautics, Vol. 169, AIAA, Washington, D.C., 1995.

[3] Oefelein, J. C., and Yang, V., "Comprehensive Review of Liquid-Propellant Combustion Instabilities in F-1 Engines," *Journal of Propulsion and Power*, Vol. 9, No. 2, 1993, pp. 657–677.

[4] Dexter, C. E., Fisher, M. E., Hulka, J. R., Denisov, K. P., Shibanov, A. A., and Agarkov, A. F., "Scaling Techniques for Design, Development and Test," *Liquid Rocket Thrust Chambers: Aspects of Modeling, Analysis and Design*, edited by V. Yang, Progress in Astronautics and Aeronautics, AIAA, Reston, VA, 2004, pp. 553–600.

[5] Sohn, C. H., and Seol, W.-S., "On the Method for Hot-Fire Modeling of High-Frequency Combustion Instability in Liquid Rocket Engines," *KSME International Journal*, Vol. 18, No. 6, 2004, pp. 1010–1018.

[6] Dranovsky, M. L., *Combustion Instability in Liquid Rocket Engines*, Progress in Astronautics and Aeronautics, Vol. 221, AIAA, Reston, VA, 2007.

[7] Crocco, L., and Cheng, S.-I., *Theory of Combustion Instability in Liquid Propellant Rocket Motors*, Butterworths Scientific, London, 1956.

[8] Summerfield, M., "Theory of Unstable Propulsion in Liquid Propellant Rocket Systems," *ARS Journal*, Vol. 21, No. 5, Sept. 1951, pp. 108–114.

[9] Lee, K.-J., Seo, S., Song, J.-Y., Han, Y.-M., Choi, H.-S., and Seol, W.-S., "Combustion Stability Assessment of Double Swirl Coaxial Injectors Using Simulant Propellants," *AIAA Joint Propulsion Conference*, AIAA Paper 2005-4443, 2005.

[10] Sohn, C. H., Seol, W. S., Shibanov, A. A., and Pikalov, V. P., "Combustion Stability Boundaries of the Subscale Rocket Chamber with Impinging Jet Injectors," *Journal of Propulsion and Power*, Vol. 23, No. 1, 2007, pp. 131–139. doi:10.2514/1.19937

[11] Cavitt, R. C., "Experimental Methodology for Measuring Combustion and Injector Coupled Responses," M.S. Thesis, Univ. of Alabama, Huntsville, AL, 2007.

D. Talley
Associate Editor